*Inorg. Chem.* **2004**, *43*, 6377−6382

# Density Functional Study of Valence Trapping in a Mixed-Valent Dimanganese Complex

**Michael Bühl* and Walter Thiel**

*Max-Planck-Institut für Kohlenforschung, Kaiser-Wilhelm-Platz 1, D-45470 Mülheim an der Ruhr, Germany*

Received May 26, 2004

Density functional calculations are reported for the linked system [(Fulv){Mn(CO)$_2$}$_2$($\mu$-dppm)] in the neutral and singly and doubly charged states. The neutral system and dication are characterized by well-localized valence states involving two Mn(II) and Mn(I) centers, respectively. At the BP86/AE1 level, the electronic structure of the monocation is that of a delocalized mixed-valence species. At the B3LYP/AE1 level, the spin density of the unpaired electron is largely localized on one Mn atom, in accord with the formulation of a trapped-valence ground state (Atwood, C. G.; Geiger, W. E. *J. Am. Chem. Soc.* **2000**, *122*, 5477). The qualitative IR pattern of the CO stretching vibrations is well reproduced at the B3LYP level, supporting the empirical charge distribution parameter employed for the interpretation of the IR spectra.

## 1. Introduction

Understanding interactions and electron transfer between metal atoms is of fundamental interest in many branches of chemistry. Mixed-valence compounds containing two or more metal centers in different oxidation states are popular model compounds for the study of electronic coupling between these centers.[1] The fundamental question is: When are electrons symmetrically distributed between the metal atoms and when are they localized on one of them? Recently, Atwood and Geiger[2] reported results for one representative of this class of compounds, [(Fulv){Mn(CO)$_2$}$_2$($\mu$-dppm)]$^+$ (**1**$^+$, Chart 1), which were interpreted in terms of a time-dependent localization process: The ESR spectrum showed characteristics of a symmetrical delocalization of the odd electron on the two Mn atoms, whereas IR spectra, which are recorded on a much faster time scale, were interpreted in terms of a localized Mn(II)/Mn(I) structure. The carbonyl stretching region, which consists of four signals instead of the two expected for a fully symmetrical, delocalized scenario, is of particular diagnostic value. Detailed analysis of the spectral shifts employing a so-called "charge distribution parameter"[3] led to the somewhat surprising conclusion of an approximately 30:70 distribution of the positive charge between the two metal fragments.[2]

**Chart 1**

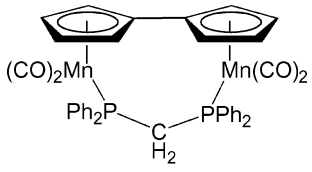


**1**

The unusual electronic structure of **1**$^+$ calls for a theoretical investigation. The modern tools of density functional theory (DFT) have matured to a point where they can afford qualitative insights and, in some cases, also quantitative answers to problems in transition metal chemistry.[4] A prerequisite for the effective application of DFT is a careful validation of the particular exchange-correlation functional for the property under scrutiny, as the choice of functional can affect the results significantly. Vibrational frequencies, specifically those of CO stretching bands in transition metal carbonyl complexes, are well described by gradient-corrected functionals such as BP86,[5] and computed IR spectra have already been applied to address dynamic phenomena in

* To whom correspondence should be addressed. E-mail: buehl@mpi-muelheim.mpg.de.

(1) For recent reviews, see for example: (a) Astruc, D. *Acc. Chem. Res*. **1997**, *30*, 383−391. (b) Barlow, S.; O'Hare, D. *Chem. Rev*. **1997**, *97*, 637−669. (c) Kaim, W.; Klein, A.; Glöckle, W. *Acc. Chem. Res.* **2000**, *33*, 755−763.

(2) (a) Atwood, G. C.; Geiger, W. E. *J. Am. Chem. Soc*. **1993**, *115*, 5310−5311. (b) Atwood, G. C.; Geiger, W. E. *J. Am. Chem. Soc*. **2000**, *122*, 5477−5485.

(3) Stoll, M. E.; Lovelace, S. R.; Geiger, W. E.; Schimanke, H.; Hyla-Kryspin, I.; Gleiter, R. *J. Am. Chem. Soc*. **1999**, *121*, 9343−9351.

(4) See, for example: Koch, W.; Holthausen, M. C. *A Chemist's Guide to Density Functional Theory*, Wiley-VCH: Weinheim, Germany, 2000 and the extensive bibliography therein.

10.1021/ic0493189 CCC: $27.50 
Published on Web 09/10/2004

carbonyl complexes with low barriers for internal rotation.[6] Because such CO bands were instrumental in the assessment of the electronic structure of $\mathbf{1}^+$, we have now computed the vibrational frequencies of the latter using suitable DFT methods. Most of the test compounds for which CO bands have been computed so far are closed-shell systems. Open-shell species such as title compound $\mathbf{1}^+$ might be less well-behaved and might pose a more pronounced challenge for the theoretical methods.[7] The purpose of this paper is thus two-fold: first, to assess representative density functionals with regard to their ability to reproduce the salient spectral features of $\mathbf{1}^+$ and, second, to contrast the electronic structure arising from the quantum-chemical calculations with that derived from the experimental observations. As it turns out, the popular hybrid functional B3LYP performs better than BP86 and supports the suggested trapped-valence model. This functional has recently also been used to study electronic coupling in a related dimanganese complex.[8]

## 2. Computational Details

Geometries were fully optimized at the RI-BP86/AE1 level, i.e., employing the exchange and correlation functionals of Becke[9] and Perdew,[10] respectively, together with a fine integration grid (75 radial shells with 302 angular points per shell); the augmented Wachters' basis[11] on Mn (8s7p4d); the 6-31G* basis[12] on all other elements except for the C atoms in the Ph moieties, for which 6-31G was used; and suitable auxiliary basis sets for the fitting of the Coulomb potential.[13] This and comparable DFT levels have proven quite successful for transition metal compounds and are well suited for the description of structures, energies, barriers, and other properties.[4] Test calculations for $Mn(Cp)(CO)_3$ at the RI-BP86 and BP86 levels (i.e., without density fitting) confirmed that geometrical parameters and CO stretching vibrations were essentially identical with the two approaches. Except for the singlet states of **1** and $\mathbf{1}^{2+}$, which were described at the restricted Kohn−Sham level, the computations employed the unrestricted Kohn−Sham formalism. Spin contamination in the latter calculations was small, with $\langle \hat{S}^2 \rangle$ values up to ca. 0.79 and 2.04 for doublet and triplet states, respectively. Harmonic frequencies were computed analytically and were used without scaling, also to obtain zero-point corrections (denoted ZPC). Unless otherwise noted, relative energies are reported without such corrections. The most stable minima were reoptimized at the B3LYP/AE1 level, that is, using the functionals according to Becke (hybrid)[14] and Lee, Yang, and Parr.[15] All computations were performed with the Gaussian 03 program package.[16]

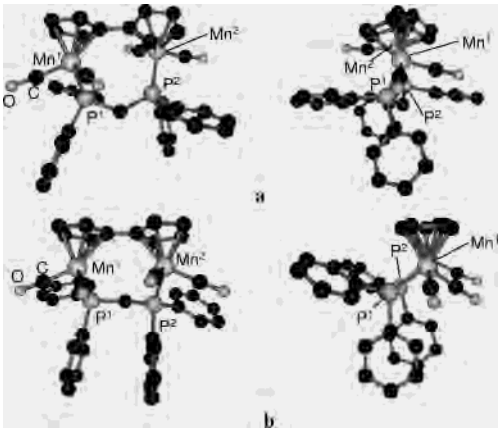


**Figure 1.** Conformations **a** (top) and **b** (bottom) of $[(Fulv)\{Mn(CO)_2\}_2(\mu\text{-dppm})]^{0/+/2+}$; two orientations are shown in each case (hydrogen atoms omitted for clarity.)

## 3. Results and Discussion

Dinuclear complexes of type **1** can exist in two conformations with a twisted (**a**) and an essentially planar fulvenyl moiety (**b**), the former entailing a larger separation between the metal nuclei (Figure 1). Conformation **a** is realized in solid, neutral **1**,[17] whereas form **b** has been characterized for $\mathbf{1}^+$ in the crystal.[2a] Optimized geometrical parameters for both conformations in the 0, +1, and +2 oxidation states are collected in Tables 1−3.

For **1a** and $\mathbf{1b}^+$, most of the BP86-optimized parameters agree quite well with the values observed in the respective solids (Tables 1 and 2). Bond lengths between Mn and P are overestimated by ca. 0.02−0.03 Å, which is typical for this level of theory. The Mn···Mn separations are even more strongly overestimated, by ca. 0.08 and 0.16 Å for **1a** and $\mathbf{1b}^+$, respectively; however, these distances are large (more than 4 Å), indicating the absence of direct bonding between the metals, and they might thus be quite sensitive to crystal-packing effects. It should also be noted that any potentially attractive dispersion forces, which would serve to draw the Mn atoms closer to one another, are missing in the employed density functionals.[4] Under these circumstances, the accord between experimental and optimized geometries can be considered satisfactory.

Whereas conformation **1a** is found to be more stable than **1b** by 4.6 kcal/mol for the neutral complex, the reverse is

(5) (a) Jonas, V.; Thiel, W. *J. Chem. Phys.* **1995**, *102*, 8474−8484. (b) Jonas, V.; Thiel, W. *J. Chem. Phys.* **1996**, *105*, 3636−3648. (c) Jonas, V.; Thiel, W. *Organometallics* **1998**, *17*, 353−360.
(6) Bühl, M.; Thiel, W. *Inorg. Chem.*, **1997**, *36*, 2922−2924.
(7) See for instance: Reiher, M. *Inorg. Chem.* **2002**, *41*, 6928−6935.
(8) Röder, J. C.; Meyer, F.; Hyla-Kryspin, I.; Winter, R. F.; Kaifer, E. *Chem. Eur. J.* **2003**, *9*, 2636−2648.
(9) Becke, A. D. *Phys. Rev. A* **1988**, *38*, 3098−3100.
(10) (a) Perdew, J. P. *Phys. Rev. B* **1986**, *33*, 8822−8824. (b) Perdew, J. P. *Phys. Rev. B* **1986**, *34*, 7406.
(11) (a) Wachters, A. J. H. *J. Chem. Phys.* **1970**, *52*, 1033−1036. (b) Hay, P. J. *J. Chem. Phys.* **1977**, *66*, 4377−4384.
(12) (a) Hehre, W. J.; Ditchfield, R.; Pople, J. A. *J. Chem. Phys.* **1972**, *56*, 2257−2261. (b) Hariharan, P. C.; Pople, J. A. *Theor. Chim. Acta* **1973**, *28*, 213−222.
(13) Generated automatically according to the procedure implemented in Gaussian 03.
(14) Becke, A. D. *J. Chem. Phys.* **1993**, *98*, 5648−5642.
(15) Lee, C.; Yang, W.; Parr, R. G. *Phys. Rev. B* **1988**, *37*, 785−789.
(16) Frisch, M. J.; Trucks, G. W.; Schlegel, H. B.; Scuseria, G. E.; Robb, M. A.; Cheeseman, J. R.; Montgomery, J. A., Jr.; Vreven, T.; Kudin, K. N.; Burant, J. C.; Millam, J. M.; Iyengar, S. S.; Tomasi, J.; Barone, V.; Mennucci, B.; Cossi, M.; Scalmani, G.; Rega, N.; Petersson, G. A.; Nakatsuji, H.; Hada, M.; Ehara, M.; Toyota, K.; Fukuda, R.; Hasegawa, J.; Ishida, M.; Nakajima, T.; Honda, Y.; Kitao, O.; Nakai, H.; Klene, M.; Li, X.; Knox, J. E.; Hratchian, H. P.; Cross, J. B.; Adamo, C.; Jaramillo, J.; Gomperts, R.; Stratmann, R. E.; Yazyev, O.; Austin, A. J.; Cammi, R.; Pomelli, C.; Ochterski, J. W.; Ayala, P. Y.; Morokuma, K.; Voth, G. A.; Salvador, P.; Dannenberg, J. J.; Zakrzewski, V. G.; Dapprich, S.; Daniels, A. D.; Strain, M. C.; Farkas, O.; Malick, D. K.; Rabuck, A. D.; Raghavachari, K.; Foresman, J. B.; Ortiz, J. V.; Cui, Q.; Baboul, A. G.; Clifford, S.; Cioslowski, J.; Stefanov, B. B.; Liu, G.; Liashenko, A.; Piskorz, P.; Komaromi, I.; Martin, R. L.; Fox, D. J.; Keith, T.; Al-Laham, M. A.; Peng, C. Y.; Nanayakkara, A.; Challacombe, M.; Gill, P. M. W.; Johnson, B.; Chen, W.; Wong, M. W.; Gonzalez, C.; Pople, J. A. *Gaussian 03*, revision B.01; Gaussian, Inc.: Pittsburgh, PA, 2003.
(17) Herrmann, W. A.; Andrejewski, D.; Herdtweck, E. *J. Organomet. Chem.* **1987**, *319*, 183−195.

**Table 1.** Optimized Bond Lengths (Å) and CO Stretching Vibrations ($cm^{-1}$) for **1**

| | **1a** | | | **1b** |
|---|---|---|---|---|
| parameter | BP86 | B3LYP | *expt*[a] | BP86 |
| $Mn^1-C(fulv)$[b] | 2.164 | 2.184 | *2.146* | 2.171 |
| $Mn^2-C(fulv)$[b] | 2.164 | 2.186 | *2.153* | 2.168 |
| $Mn^1-C(O)$[b] | 1.776 | 1.788 | *1.772* | 1.775 |
| $Mn^2-C(O)$[b] | 1.774 | 1.786 | *1.778* | 1.778 |
| $Mn^1-P^1$ | 2.246 | 2.276 | *2.228* | 2.237 |
| $Mn^2-P^2$ | 2.253 | 2.294 | *2.263* | 2.265 |
| Mn···Mn | 4.663 | 4.667 | *4.588* | 4.477 |
| C−C(fulv) | 1.476 | 1.473 | *1.477* | 1.471 |
| $\theta$(CCCC)[c] | 61.5 | 58.6 | *64.5* | −9.2 |
| $\nu_{CO}$[d] | 1879 (0.5) | 1956 (0.6) | | 1896 (0.8) |
| | 1899 (0.9) | 1981 (1.0) | *1861 (0.9)* | 1914 (0.2) |
| | 1941 (1.0) | 2025 (1.0) | *1934 (1.0)* | 1940 (0.9) |
| | 1948 (0.4) | 2035 (0.5) | | 1955 (1.0) |

[a] Geometric parameters from ref 17; IR data from ref 2 (intensities estimated from plotted spectrum). [b] Average value. [c] Dihedral angle across the fulvalene bridge (average of two values that would be identical if the fulvalene moiety had local $C_2$ symmetry). [d] Relative intensities in parentheses.

**Table 2.** Optimized Bond Lengths (Å) and CO Stretching Vibrations ($cm^{-1}$) for $\mathbf{1}^+$

| | $\mathbf{1a}^+$ | $\mathbf{1b}^+$ | | |
|---|---|---|---|---|
| parameter | BP86 | BP86 | B3LYP | *expt*[a] |
| $Mn^1-C(fulv)$[b] | 2.177 | 2.172 | 2.190 | *2.140* |
| $Mn^2-C(fulv)$[b] | 2.175 | 2.172 | 2.187 | *2.140* |
| $Mn^1-C(O)$[b] | 1.797 | 1.796 | 1.800 | *1.801* |
| $Mn^2-C(O)$[b] | 1.794 | 1.798 | 1.846 | *1.791* |
| $Mn^1-P^1$ | 2.300 | 2.297 | 2.294 | *2.268* |
| $Mn^2-P^2$ | 2.312 | 2.315 | 2.396 | *2.279* |
| Mn···Mn | 4.581 | 4.231 | 4.264 | *4.070* |
| C−C(fulv) | 1.462 | 1.458 | 1.453 | *1.436* |
| $\theta$(CCCC)[b] | 44.3 | −6.2 | −8.3 | *−3.6* |
| $\nu_{CO}$[c] | 1915 (0.3) | 1928 (0.0) | 1986 (0.2) | *1888 (0.5)* |
| | 1942 (0.1) | 1957 (0.2) | 2040 (1.0) | *1931 (1.0)* |
| | 1967 (1.0) | 1967 (1.0) | 2081 (0.3) | *1952 (0.3)* |
| | 1994 (0.1) | 1996 (0.3) | 2105 (0.6) | *2003 (0.7)* |

[a] From ref 2 (intensities estimated from plotted spectrum). [b] Average value. [c] Relative intensities in parentheses.

**Table 3.** Optimized Bond Lengths (Å) and CO Stretching Vibrations ($cm^{-1}$) for $\mathbf{1}^2$

| | $^3\mathbf{1a}^{2+}$ | $^1\mathbf{1b}^{2+}$ | $^3\mathbf{1b}^{2+}$ | | |
|---|---|---|---|---|---|
| parameter | BP86 | BP86 | BP86 | B3LYP | *expt*[a] |
| $Mn-C(fulv)$[b] | 2.186 | 2.175 | 2.189 | 2.200 | |
| $Mn-C(O)$[b] | 1.822 | 1.811 | 1.822 | 1.865 | |
| $Mn^1-P^1$ | 2.332 | 2.350 | 2.345 | 2.387 | |
| $Mn^2-P^2$ | 2.356 | 2.350 | 2.336 | 2.412 | |
| Mn···Mn | 4.614 | 3.724 | 4.360 | 4.383 | |
| C−C(fulv) | 1.476 | 1.445 | 1.468 | 1.469 | |
| $\theta$(CCCC)[b] | 54.3 | 0.0 | 3.6 | −8.3 | |
| $\nu_{CO}$[c] | 1949 (0.6) | 1972 (0.0) | 1967 (0.1) | 2085 (0.4) | *1990 (0.1)* |
| | 1977 (0.8) | 1998 (0.2) | 1990 (0.2) | 2109 (0.5) | *2007 (0.3)* |
| | 2020 (1.0) | 2014 (1.0) | 2017 (1.0) | 2141 (1.0) | *2025 (1.0)* |
| | 2034 (0.7) | 2031 (0.5) | 2029 (0.6) | 2152 (0.7) | *2053 (0.9)* |

[a] From ref 2 (intensities estimated from plotted spectrum). [b] Average value. [c] Relative intensities in parentheses.

found for the monocation, where $\mathbf{1a}^+$ lies 3.8 kcal/mol above $\mathbf{1b}^+$ (zero-point corrections reduce these numbers slightly, to 4.2 and 3.6 kcal/mol, respectively). These BP86 results are fully consistent with the observed conformational preferences and suggest that, for each species, the equilibrium mixture consists essentially of one isomer. Also, no interconversion between forms **a** and **b** is to be expected on the IR time scale.

The situation is less clear-cut for the dication, which can exist as a triplet or as a singlet with, respectively, ferromagnetic and antiferromagnetic coupling between two low-spin Mn(II) centers. For conformation $\mathbf{1a}^{2+}$ with the more distant metal centers, singlet and triplet are energetically degenerate at the UBP86 level and afford essentially identical structural and IR vibrational parameters. As the open-shell singlet is ill-described with a single UKS determinant, which is plagued by substantial spin contamination ($\langle\hat{S}^2\rangle \approx 1.0$ rather than 0), only the results for triplet $\mathbf{1a}^{2+}$ are given in Table 3. For conformation $\mathbf{1b}^{2+}$, starting from the geometry of $\mathbf{1b}^+$, the singlet state described by an unrestricted wave function converges to the closed-shell solution, and the geometry optimizes to effective $C_s$ symmetry. At the BP86 level, the triplet is higher in energy than the singlet by 6.5 kcal/mol. However, single-point energy calculations at the B3LYP level reverse the energetic ordering, placing $^3\mathbf{1b}^{2+}$ 12.1 kcal/mol below $^1\mathbf{1b}^{2+}$ and 0.9 kcal/mol below $^3\mathbf{1a}^{2+}$. Relative stabilities of different spin states of open-shell transition metal complexes are a notorious problem for DFT and can vary radically from one functional to another.[4,7] From the energetic results, no definite conclusions regarding spin state and conformation can be drawn for $\mathbf{1}^{2+}$. For the discussion of the IR properties below, however, it is worth noting that the predicted CO stretching bands (lower part of Table 3) are qualitatively quite similar for each of the isomeric dications considered. Incidentally, the intensities computed for $^3\mathbf{1b}^{2+}$, the lowest form according to B3LYP, fit best to the observed spectrum. Because the dication is not the main target of the present study, we refrain from a more sophisticated, quantitative analysis[18] and use, without further substantiation, the results obtained for $^3\mathbf{1b}^{2+}$ to describe the dication. Likewise, we will evaluate only the results for **1a** and $\mathbf{1b}^+$ when discussing the neutral and the monocation, respectively, and drop the labels **a** and **b** henceforth.

Turning now to the electronic structure of $\mathbf{1}^+$, analysis of the BP86 density indicates an almost perfect delocalization of the unpaired electron between the two metal fragments. The highest (singly) occupied MO (HOMO) is located to essentially equal parts on these fragments, and the computed spin densities at the Mn atoms are 0.46 and 0.49, that is, the two values are very similar and close to 0.5. As a consequence, population analyses (both Mulliken and natural population analysis, NPA)[19] afford negligible charge separation between the two moieties.

The schematic IR spectra of the carbonyl region computed at the RI-BP86/AE1 level are depicted in Figure 2b and compared to the experimental one in Figure 2a. Four distinct bands with nonvanishing intensities are predicted for all oxidation states, including **1** and $\mathbf{1}^{2+}$, in which the two metal atoms have the same electronic configuration. Thus, from

(18) For instance using the popular broken-symmetry approach; for a recent review, see: Ciofini, I.; Daul, C. *Coord. Chem. Rev.* **2003**, *238*−*239*, 187−209.

(19) Reed, A. E.; Curtiss, L. A.; Weinhold, F. *Chem. Rev.* **1988**, *88*, 899−926.

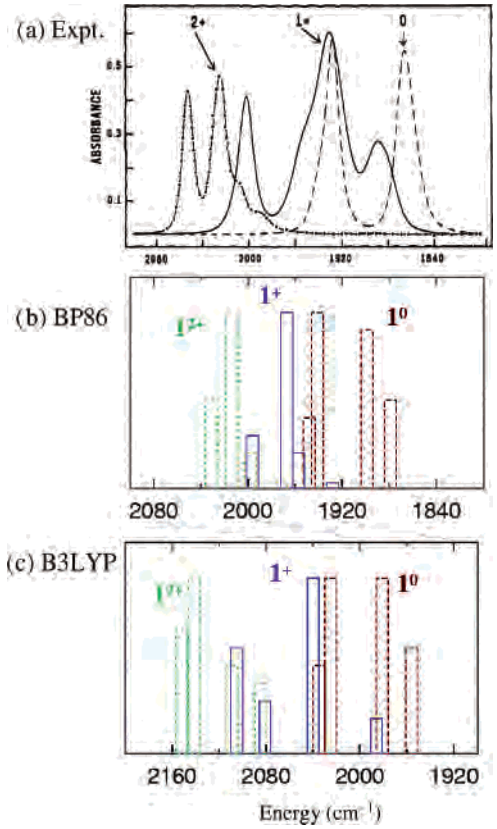


**Figure 2.** IR bands from the carbonyl stretching regions of **1**, $\mathbf{1}^{+}$ and $\mathbf{1}^{2+}$: (a) experiment (reprinted with permission from ref 2a; copyright 1993 American Chemical Society); (b) BP86/AE1, schematic; (c) B3LYP/AE1, schematic, axis red-shifted by 70 $cm^{-1}$. Computed spectra for the neutral species, the monocation, and the dictation are rendered in red, blue, and green, respectively.

the occurrence of four signals alone, one cannot draw any conclusions regarding the charge or spin distribution between the metal centers. For neutral **1**, where just two lines are observed, each peak might consist of two close-lying signals that are not resolved because of the notable line widths. In fact, the two bands at higher frequency are computed to differ only by 7 $cm^{-1}$, whereas a somewhat larger separation, 20 $cm^{-1}$, is predicted for the pair of bands at lower frequency (see Table 1 for the values). The latter value is of the same order as the line width of the observed resonances (at half-height) and should, in principle, be detectable, at least in the form of a shoulder. Such small differences in energy, however, are certainly within the error margin of the theoretical methods used, and the computed and observed IR patterns appear to be consistent with each other. The separation of the two principal bands is fairly well reproduced computationally, 55 $cm^{-1}$ (difference between the pairwise-averaged high- and low-frequency bands), as compared to the experimental value of 73 $cm^{-1}$.

Also for the dication $\mathbf{1}^{2+}$, the computed and observed patterns agree fairly well. The BP86 data afford low intensities for the two low-frequency modes, which are recognizable as shoulders in the experimental spectrum (see the leftmost part in Figure 2a, labeled 2+). The total span of the peaks, that is, the difference ($\Delta$) between the two outermost ones, is very well described theoretically, $\Delta =$ 62 $cm^{-1}$, as compared to experiment, $\Delta = 63$ $cm^{-1}$. As for the absolute values of the computed vibrational modes, those of **1** appear to be slightly shifted to higher frequencies compared to their experimental counterparts, whereas those of $\mathbf{1}^{2+}$ appear at somewhat lower values. The overall blue shift of the bands upon double oxidation of **1** is thus underestimated in the computations, but the trend is well captured qualitatively.

Unlike for **1** and $\mathbf{1}^{2+}$, experimental and BP86 IR patterns do not match well for the title compound, $\mathbf{1}^{+}$ (see Figure 2a and b). In particular, the computed span, $\Delta = 68$ $cm^{-1}$, is very similar to that of **1** or $\mathbf{1}^{2+}$ and much smaller than the observed value, $\Delta = 115$ $cm^{-1}$. Thus, the experimental spectrum is not reproduced at the BP86 level with the symmetrical mixed-valence electronic structure.

To probe the extent to which the DFT results depend on the exchange-correlation functional, we reoptimized **1**, $\mathbf{1}^{+}$, and $\mathbf{1}^{2+}$ at the B3LYP/AE1 level and computed the harmonic frequencies. On going from BP86 to B3LYP, most distances involving Mn increase noticeably, thereby worsening the agreement with experiment (see Tables 1 and 2). This is in keeping with occasional findings that B3LYP is not necessarily superior to pure, gradient-corrected functionals in terms of the geometries of transition metal complexes.[20] Compared to BP86, the B3LYP harmonic frequencies are shifted to higher values, which, in an absolute sense, appear to fit less well to experiment. Because the latter values refer to (anharmonic) fundamentals, however, such a shift is to be expected, and the good agreement between the BP86 harmonic and experimental fundamental frequencies that is usually found benefits from error cancellation. Because relative trends are more important than absolute values, we have shifted the B3LYP spectrum in Figure 2c by a constant amount for comparison with experiment (by ca. 70 $cm^{-1}$, compare parts a and c of Figure 2).[21]

This offset notwithstanding, only minor changes are found in the appearance of the spectra of **1** and $\mathbf{1}^{2+}$ on going from BP86 to B3LYP (compare parts b and c of Figure 2). In contrast, the pattern predicted for $\mathbf{1}^{+}$ changes drastically: Not only the intensity pattern is modified such that it fits well to the observed one, but also a much larger span is obtained at the B3LYP level, $\Delta = 119$ $cm^{-1}$ (Table 1), in almost perfect agreement with experiment. Except for a minor detail, namely, the exact position of the second-highest band with respect to its neighboring ones, the qualitative features of the experimental spectrum are very well captured at the B3LYP level.

Analysis of the B3LYP results for $\mathbf{1}^{+}$ reveals a possible reason for the qualitatively different predictions of the IR spectrum compared to the BP86 data: The two functionals yield completely different descriptions of the electronic structure. Whereas BP86 predicts an essentially symmetrical mixed-valence compound, B3LYP affords a highly unsym-

(20) See, for example: (a) Hamprecht, F. A. H.; Cohen, A. J.; Tozer, D. J.; Handy, N. C. *J. Chem. Phys.* **1998**, *109*, 6264−6271. (b) Barden, C. J.; Rienstra-Kiracofe, J. C.; Schaefer, H. F. *J. Chem. Phys.* **2000**, *113*, 690−700.

(21) Alternatively, one can scale the computed harmonic frequencies; see: Yu, L.; Srinivas, G. N.; Schwartz, M. *J. Mol. Struct. (THEOCHEM)* **2003**, *625*, 215−220.

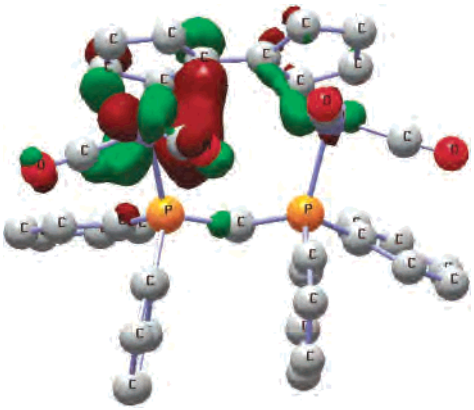

**Figure 3.** Highest singly occupied MO in $\mathbf{1}^+$ at the B3LYP/AE1 level.

metric, trapped-valence state.[22] The HOMO depicted in Figure 3 clearly shows that the odd electron is localized to a large extent on one of the Mn atoms. Similarly, B3LYP gave a localized description in a related pyrazolate-bridged dimanganese complex.[8] More quantitatively, the computed Mulliken spin densities on the two Mn atoms in $\mathbf{1}^+$ are 0.20 and 0.92. Concomitant with spin localization, appreciable charge separation $\Delta q$ is found. Total Mulliken charges on the two centers are $-0.40$ and $-0.24$, implying $\Delta q = 0.16$. The corresponding values from natural population analysis are $-0.47$ and $-0.17$, with $\Delta q = 0.30$. Incidentally, the latter value is almost identical to the experimental estimate of $\Delta q = 0.29$.[2b] Although this apparent agreement should not be overinterpreted, it is clear that B3LYP with its trapped-valence description of $\mathbf{1}^+$ can reproduce the experimental IR spectrum, whereas BP86 with its symmetrical mixed-valence structure cannot. The interpretation of the observed IR data in terms of a trapped-valence species is thus fully corroborated by our theoretical data.[23]

An intriguing aspect of the chemistry of $\mathbf{1}^+$ is that valence trapping can only be detected by very fast spectroscopic methods such as IR and not by, for instance, ESR, which probes longer time scales. This observation, which has been termed "time-dependent valence detrapping",[2a] is consistent with a low barrier for hopping of the odd electron (or, in an alternative description, a hole in a $d^6$ subshell) from one Mn center to the other, presumably via a transition state with symmetrical mixed-valence character. One way to model such a state is to enforce it by imposing $C_s$ symmetry. Because of conformational preferences of the Mn($\mu$-dppe)-Mn backbone, the two metal fragments in the ground state of $\mathbf{1}^+$ are not mirror images of each other, and the overall symmetry is $C_1$ (even at the BP86 level). Optimization under the constraint of $C_s$ symmetry yields a stationary point that turns out to be a transition state for rearrangement of $\mathbf{1}^+$ to its enantiomer. The barrier for this process is 0.5 and 0.7 kcal/mol at the BP86/AE1 and B3LYP/AE1 levels,[24] respectively (0.2 and 0.1 kcal/mol, respectively, with inclusion of zero-point corrections). Indeed, barriers this low would be consistent with the experimental observations. Interestingly, the B3LYP barrier is not much higher than that computed at the BP86 level, even though the electronic structure at the former level changes on going from the minimum to the transition state, whereas it stays the same with the latter functional.

The change in electronic structure in the B3LYP transition state is also reflected in the CO stretching vibrations, which are computed to appear at 1952 (1.0), 2052 (0.3), 2059 (0.0), and 2093 (0.1) $cm^{-1}$ (relative intensities in parentheses). This pattern (in particular, that of the intensities) is very different from the B3LYP data given for the minimum in Table 2 and is not compatible with the observed spectrum.[25] This result can be taken as further evidence that the B3LYP minimum with its trapped-valence nature is correct and argues against a symmetrical mixed-valence structure of $\mathbf{1}^+$.

Theoretical studies of mixed-valence transition metal complexes have a long history, and for a proper description of all spectroscopic properties, particularly the charge-transfer band associated with electron transfer between the metal centers, it can be necessary to go beyond the Born−Oppenheimer approximation.[26] The same can be true for quantitative aspects of the valence detrapping dynamics,[27] but the qualitative conclusion from the computations, namely, that this should be a very rapid process, is entirely reasonable.

Another problem that can be crucial for DFT studies of the mixed-valence/trapped-valence dichotomy and that, to our knowledge, has received only little attention so far, is the spurious self-interaction inherent to all common density functionals.[4,28] This effect can be particularly important in charged odd-electron systems, a prominent example being

(22) The symmetrical electronic structure with BP86 is not an artifact of an accidentally symmetrical initial guess, but is recovered when starting the BP86 optimization of wave function and geometry from the unsymmetrical B3LYP minimum.

(23) No effects of solvent and counterions are included in the computations discussed so far. We have assessed bulk medium effects by performing single-point energy calculations using a polarizable continuum model (as implemented in Gaussian 03, cf. Cossi, M.; Scalmani, G.; Rega, N.; Barone, V. *J. Chem. Phys.* **2002**, *117*, 43 and references therein) using the parameters of dichloromethane: upon inclusion of the continuum, the spin distribution is unchanged with BP86 and is only slightly shifted to a more pronounced localization with B3LYP (spin density 0.15:0.97). It is thus unlikely that bulk solvation would induce significant changes in the appearance of the IR spectra. Finer details of the latter could be affected by ion pairing; a comprehensive study of these effects, i.e., specific inclusion of $BF_4^-$ counterions, is beyond the scope of this paper.

(24) The B3LYP wave function of the symmetrical form is stable in $C_s$ symmetry, and no lower symmetry-broken solution was found.

(25) It is noteworthy that the span of the CO vibrations is large at the B3LYP level both for the localized minimum (119 $cm^{-1}$) and for the $C_s$-symmetrical transition state (141 $cm^{-1}$), whereas it is small at the BP86 level in each case (68 and 67 $cm^{-1}$, respectively). Hence, the calculated span is affected by the extent of spin localization and by the chosen functional. In view of this situation, our conclusions are based not only on these spans, but mainly on the overall appearance of the spectrum (frequency and intensity patterns; see text).

(26) See, for example: (a) Piepho, S. B. *J. Am. Chem. Soc.* **1988**, *110*, 6319−6326. (b) Schatz, P. N. In *Inorganic Electronic Structure and Spectroscopy*; Solomon, E. I.; Lever, A. B. P., Eds.; John Wiley & Sons: New York, 1999; Vol. II: Applications and Case Studies, pp 175−226 and references therein.

(27) Because of vibronic coupling, the actual rate of electron transfer in the title compound might be somewhat lower than suggested by the very low barrier of only fractions of a kilocalorie per mole computed on the Born−Oppenheimer surface; otherwise, dynamic effects (coalescence) might be expected in the room-temperature IR spectrum of $\mathbf{1}^+$. For dynamic IR spectroscopy of mixed-valent compounds, see: Londergan, C. H.; Kubiak, C. P. *Chem. Eur. J.* **2003**, *9*, 5962−5969.

the stretching potential of $X_2^+$ (X = H or He):[29] At large distances, the exchange energy approximated from the density functional can no longer compensate for the Coulomb repulsion (as it would in the perfectly self-interaction-free case), and the total energy of the system is artificially lowered, eventually converging to that of a symmetrical $X^{(1/2)+}\cdots X^{(1/2)+}$ state. It is quite possible that, for $\mathbf{1}^+$ with its large Mn···Mn separation, the "pure" BP86 functional erroneously prefers a corresponding $Mn^{(3/2)+}\cdots Mn^{(3/2)+}$ configuration, that is, the symmetrical mixed-valence description, for the same reason.[30] . Admixture of Hartree−Fock exchange in the hybrid functional partly alleviates this problem, because the Hartree−Fock method itself is self-interaction-free. This feature could explain the different performances of the two DFT methods. B3LYP is not free of self-interaction error, however, and it is quite possible that, at even larger metal−metal separations, a symmetrical mixed-valence solution could arise as an artifact. Judging from its good performance for $\mathbf{1}^+$, B3LYP appears to be the method of choice for the study of mixed-valence transition metal complexes, but it might not be infallible without explicit self-interaction correction.

## Conclusions

The mixed-valence/trapped-valence dichotomy in $\mathbf{1}^+$, and presumably in other related dinuclear transition metal complexes as well, is a problem for current approximate density functional theory. Different exchange-correlation functionals can favor either a localized or a delocalized description of the electronic structure. For $\mathbf{1}^+$, the pure gradient-corrected BP86 functional predicts a delocalized mixed-valence state, whereas the B3LYP hybrid functional affords a trapped-valence structure, with the odd electron essentially localized on one Mn atom. The observed IR pattern of the carbonyl stretching region, which is very sensitive to the interaction between the metal centers, is qualitatively reproduced at the B3LYP level, but not at the BP86 level, thus lending support to the trapped-valence description of the cation. A $C_s$-symmetric transition state for degenerate rearrangement, in which a delocalized mixed-valence state is enforced, is predicted to be only a few tenths of a kilocalorie per mole higher in energy. The latter finding is consistent with the observed apparent time dependence of the charge-localization phenomenon, which can be detected only with very fast spectroscopical methods.

**Acknowledgment.** This work was supported by the Deutsche Forschungsgemeinschaft. We thank Prof. F. A. Cotton for bringing the problem to our attention and Prof. W. Geiger, Dr. F. Neese, and Dr. S. Patchkovskii for stimulating discussions. Computations were performed on Compaq XP1000 and ES40 workstations at the MPI Mülheim.

IC0493189

(28) See also: (a) Perdew, J. P.; Zunger, A. *Phys. Rev. B* **1981**, *23*, 5048−5079. (b) Grafenstein, J.; Kraka, E.; Cremer, D. J. *J. Phys. Chem. A* **2004**, *108* (20), 524−539.

(29) Merkle, R.; Savin, A.; Preuss, H. *J. Chem. Phys*. **1992**, *97*, 9216−9221.

(30) Self-interaction correction usually improves the description of magnetic exchange interactions in solid materials containing transition metals; see for example: Svane, A.; Gunnarsson, O. *Phys. Rev. Lett.* **1990**, *65*, 1148−1151.